Design of the IMP microbeam irradiation system for 100 MeV/u heavy ions[*]

SHENG Li-Na(盛丽娜)[1,2;1]　　SONG Ming-Tao(宋明涛)[1]　　ZHANG Xiao-Qi(张小奇)[1]

YANG Xiao-Tian(杨晓天)[1]　　GAO Da-Qing(高大庆)[1]　　HE Yuan(何源)[1]　　ZHANG Bin(张斌)[1]

LIU Jie(刘杰)[1]　　SUN You-Mei(孙友梅)[1]　　DANG Bing-Rong(党秉荣)[1]　　LI Wen-Jian(李文建)[1]

SU Hong(苏弘)[1]　　MAN Kai-Di(满开第)[1]　　GUO Yi-Zhen(郭艺珍)[1]

WANG Zhi-Guang(王志光)[1]　　ZHAN Wen-Long(詹文龙)[1]

1 (Institute of Modern Physics, Chinese Academy of Sciences, Lanzhou 730000, China)
2 (Graduate University of Chinese Academy of Sciences, Beijing 100049, China)

Abstract A state-of-the-art high energy heavy ion microbeam irradiation system is constructed at the Institute of Modern Physics of the Chinese Academy of Sciences. This microbeam system operates in both full current intensity mode and single ion mode. It delivers a predefined number of ions to pre-selected targets for research in biology and material science. The characteristic of this microbeam system is high energy and vertical irradiation. A quadrupole focusing system, in combination with a series of slits, has been designed to optimize the spatial resolution. A symmetrically achromatic system leads the beam downwards and serves simultaneously as an energy analyzer. A high gradient quadrupole triplet finally focuses a C^{6+} ion beam to 1 μm in the vacuum chamber within the energy range from 10 MeV/u to 100 MeV/u. In this paper, the IMP microbeam system is described in detail. A systematic investigation of the ion beam optics of this microbeam system is presented together with the associated aberrations. Comparison is made between the IMP microbeam system and the other existing systems to further discuss the performance of this microbeam. Then the optimized initial beam parameters are given for high resolution and high hitting efficiency. At last, the experiment platform is briefly introduced.

Key words microbeam, high energy, ion beam optics, aberration

PACS 41.85.Gy, 41.85.Ja, 41.85.Lc

1　Introduction

An ion microbeam system is a powerful tool for material and biology research at micrometer or sub-micrometer dimensions. At present, there are many microbeam facilities all over the world, and most of them use low energy light particles. The laboratories having heavy ion microbeams are JAERI and GSI with maximum energy 27.5 MeV/u and 11.4 MeV/u, respectively. With further research on astronautics, the current trend in microbeam facilities is to develop higher energy heavy ion microbeams with better spatial resolution, permitting the investigation of an important unanswered question: whether neurons that survive traversal by highly charged, high energy particles develop changes as a late consequence of the damage they incurred[1]. In addition, a high energy heavy ion beam is very useful in breeding with mutation inducement[2] and elucidating the mechanism of single event phenomena in semiconductor devices for space craft[3].

A state-of-the-art heavy ion microbeam irradiation system is under development at the Institute of Modern Physics (IMP) of the Chinese Academy of Sciences (CAS). The aim is to irradiate materials in vacuum and living cells in atmosphere at different foci with an exact number of ions targeting an area of sub-micron scale. The advantage of this system is

that the beam energy is up to 100 MeV/u for C ions. Vertical irradiation is another advantage, especially for cells irradiation. It reduces the problems associated with cell movement under gravity and hence the overall target complexity as compared with a horizontal system[4].

In the design of the IMP microbeam with a high accuracy, focusing using quadrupole magnets has been proposed as an alternative to the usually employed collimating. This solution improves the targeting accuracy and allows a faster irradiation since the beam may be positioned by means of a fast deflection system[5]. At laboratories around the world there are many configurations of quadrupole magnets arranged in different ways to focus the ion beam. The most common systems are doublet, triplet and quadruplet, but even a quintuplet exists[6]. A high precision magnetic quadrupole triplet is adopted in the IMP microbeam system. This focusing system creates a demagnified image of the object aperture, and also suffers from aberrations, i.e. the image becomes broadened or deformed.

2   Design of the IMP microbeam system

The IMP high energy heavy ion microbeam system is based on the Heavy Ion Research Facility in Lanzhou (HIRFL), which delivers heavy ion beams ranging from C to U. The microbeam line μ-beam is situated at the basement of the experiment hall.

The scheme of the IMP microbeam system is shown in Fig. 1[7]. The ions enter the microbeam end-station after two dipole magnets (R1B1 and R0B0) with 50° and 30°, respectively. The ion beam passing the object slit is focused by three quadrupole magnets (R0Q1—R0Q3) with a bore diameter of 80 mm. The object slit with an aperture from 0 to 150 μm and the following two slits are all made by Technisches Buro S. Fischer. The ion beam is deflected downwards by a symmetrically achromatic system, composed of two identical 45° dipole magnets (R0B1 and R0B2) and a quadrupole magnet R0Q4 with a bore diameter of 80 mm in between. A divergence defining slit, defining the divergence angle and the momentum spread of the beam simultaneously, is situated just before the second dipole magnet. The two 45° dipole magnets and the divergence defining slit make an energy analyzer. At last, the ion beam is strongly focused to the micron scale on a target using a high gradient quadrupole triplet (R0Q5—R0Q7) with a bore diameter of 15 mm and a maximum pole field of 1.0 T. All the magnetic elements are designed by the microbeam group, and fabricated in Lanzhou except for the high gradient quadrupole triplet. The anti-scattering slit, set before the quadrupole triplet, prevents the scattered ions from entering the quadrupole triplet. A silicon nitride vacuum window (thickness of 200 nm) at the end of the beam line is used to extract the beam into the atmosphere to irradiate living cells with micron scale, which is verified by the ANSYS and SRIM[8] codes. The samples in air are set as close as possible to the vacuum window (about 50—100 μm) to reduce the effect of beam scattering. The number of the delivered ions is controlled by electrostatic deflector plates (beam switch) to switch the
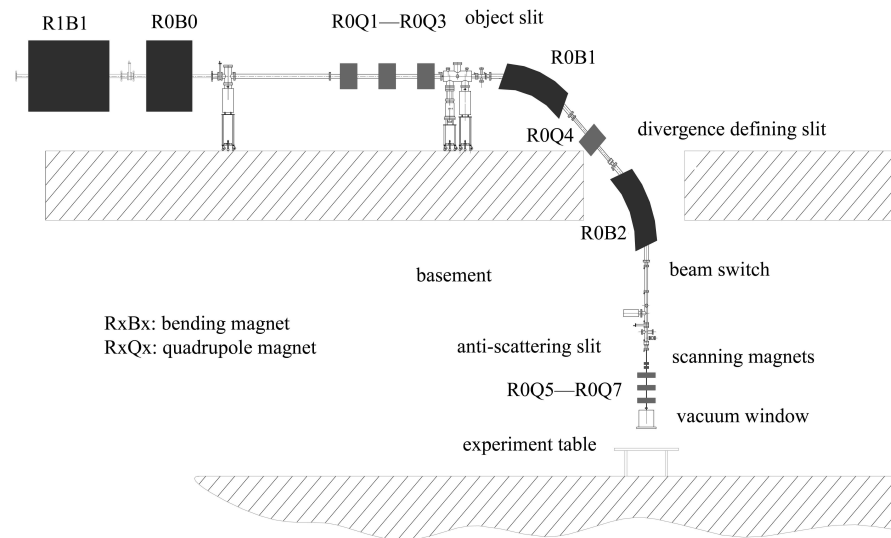

Fig. 1.　Scheme of the IMP microbeam system.

beam on and off. A fast 2-D ion scanning system is used for spot scanning or raster scanning, so that a large number of samples can be irradiated in a short time. Three sets of fluorescent and faraday cup probes near the slits are used to observe the beam profile.

3　Calculation of ion beam optics

The ion beam optical property for the IMP microbeam system is calculated by the computer codes MULE, MIRKO[9] and TRANSPORT integrated in PBO-LAB[10]. The other codes are usually used to simulate a straight beam line, e.g. PRAM, TRAX, GEANT4[11]. C^{6+} ions with energy of 80 MeV/u are taken as an example in the following calculations. All the simulations and calculations in this paper are beginning from the object slit. In Fig. 2, the ion beam optics of the IMP focusing system is shown.
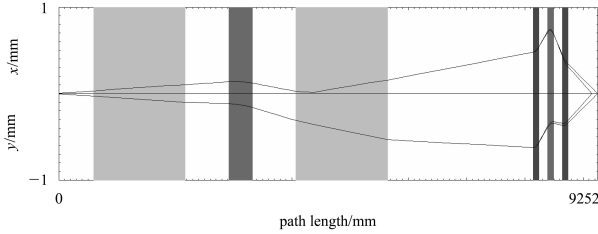

Fig. 2. Ion beam optics of the IMP focusing system with two foci by the MIRKO code.

3.1　Intrinsic aberrations

The magnetic quadrupole triplet is the key part of the IMP microbeam, designed in Lanzhou and fabricated in Shanghai, configured into either Converge,

Diverge and Converge (CDC) or Diverge, Converge and Diverge (DCD). Note that, all results given below are calculated from the CDC configuration except Table 1. The magnetic focusing system creates a demagnified image of the object aperture in the image plane, and also suffers from intrinsic and parasitic aberrations which will broaden the beam spot. There are three dominant types of aberrations in a quadrupole focusing system[12]: chromatic aberration (due to the beam momentum spread), spherical aberration (caused by fringe quadrupole field effects) and parasitic aberration (due to mechanical imperfections in the lenses or the system). The resulting beam spot size depends strongly on the demagnification factor and the correction of these aberrations in the focusing system, which can be shown by the expression of the position of an ion in a focusing microbeam system[13],

$$x_i = \langle x|x\rangle x_o + \langle x|\theta\rangle\theta_o + \langle x|\theta\delta\rangle\theta_o\delta_o +$$
$$\langle x|\theta^3\rangle\theta_o^3 + \langle x|\theta\Phi^2\rangle\theta_o\Phi_o^2 + \cdots , \quad (1)$$

$$y_i = \langle y|y\rangle y_o + \langle y|\Phi\rangle\Phi_o + \langle y|\Phi\delta\rangle\Phi_o\delta_o +$$
$$\langle y|\Phi^3\rangle\Phi_o^3 + \langle y|\theta^2\Phi\rangle\theta_o^2\Phi_o + \cdots , \quad (2)$$

where $(x_o, \theta_o, y_o, \Phi_o)$ represents the position and divergence angle of a beam particle in the object plane, δ_o is the particle momentum relative to the mean momentum, the demagnification of the system is $\langle x|x\rangle^{-1}$ and $\langle y|y\rangle^{-1}$ in the image plane, $\langle x|\theta\rangle$ and $\langle y|\Phi\rangle$ are the astigmatism coefficients, $\langle x|\theta\delta\rangle$ and $\langle y|\Phi\delta\rangle$ are the chromatic aberration coefficients, and $\langle x|\theta^3\rangle$, $\langle x|\theta\Phi^2\rangle$, $\langle y|\Phi^3\rangle$ and $\langle y|\theta^2\Phi\rangle$ are the spherical aberration coefficients. In a well-focused system, the astigmatism coefficients are zero.

Table 1. Beam optical parameters for the IMP CDC and DCD configurations and some existing microbeam facilities.

	IMP(CDC)	IMP(DCD)	PTB[A]	Oxford[B]	Oxford[C]
ion species	C^{6+}	C^{6+}	proton, ^{4}He	proton	proton
energy/MeV	960	960	0.5—20, 1.0—28	4	4
D_x	15.19	16.07	7.8	60.55	67.80
D_y	−15.20	−17.37	20	−14.13	−15.21
chromatic aberration coefficients/(μm/(mrad%))					
$\langle x|\theta\delta\rangle$	−329.7	−129.6	160.0	−258.5	−246.31
$\langle y|\Phi\delta\rangle$	182.0	443.2	70.0	774.4	782.97
spherical aberration coefficients/(μm/mrad^3)					
$\langle x|\theta^3\rangle$	175.1	16.89	–	–	87.92
$\langle x|\theta\Phi^2\rangle$	166.0	188.0	–	–	111.1
$\langle y|\Phi^3\rangle$	−33.71	−378.8	–	–	−437.9
$\langle y|\theta^2\Phi\rangle$	−165.9	−173.9	–	–	−427.6
figure of merit Q	12.78	15.04	–	–	30.54

A: PTB quadrupole doublet[14] calculated by TRANSPORT code. B: Oxford University quadrupole triplet[15] with A-AB configuration calculated by TRANSPORT code. C: Oxford University quadrupole triplet[16] with A-AB configuration calculated by OXRAY code.
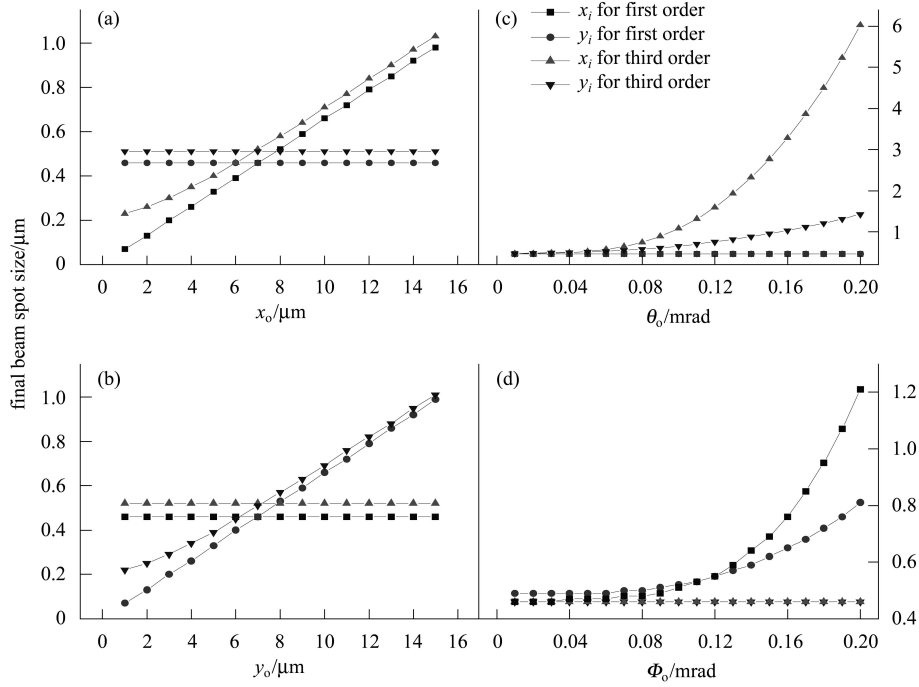
Fig. 3.   The final beam spot size against the object size x_o, y_o and the divergence angle θ_o, Φ_o.

Some physical parameters and the dominant aberration coefficients for the IMP microbeam system as calculated by the TRANSPORT and MULE codes are shown in Table 1. For comparison, the corresponding parameters and aberration coefficients of some existing microbeam facilities are also tabulated. The figure of merit of the system[16], Q factor, is also given. This factor which combines the demagnifications and spherical aberration terms is defined as follows. Usually, a system with a large value of Q potentially offers superior performance.

$$Q = \frac{D_x \cdot D_y}{\sqrt[3]{\langle x|\theta^3 \rangle \cdot \langle y|\phi^3 \rangle}} \ . \tag{3}$$

Figure 3 shows the variation of the final beam spot size with the object sizes and the divergence angles. In this calculation, only one initial beam parameter is varying at any plot. From Fig. 3 two conclusions can be drawn. First, the beam spot size risies linearly whether first order or third order with the increase of the object size from (a) and (b), but x_i for the third order is more sensitive than y_i to the change in object size. Secondly, the divergence angles have no effect on the beam spot size for the first order but more effects for the third order from (c) and (d). In addition, the divergence angle θ_o contributes to x_i and y_i for the third order, which is similar to Φ_o.

Suppression of focusing errors, induced by spherical and chromatic aberrations in the quadrupole focusing system, is very significant for the microbeam production. Precise fabrication and alignment of the magnets are required for the suppression of spherical aberrations. Minimization of the momentum spread of the beam is essential for reduction of the chromatic aberrations. Table 2 shows the simulations for the optimized initial beam parameters to attain a 1 μm beam spot size in the vacuum chamber.

Table 2.   Optimized initial beam parameters for the CDC and DCD configurations for a 1 μm beam spot.

initial beam parameters	CDC configuration	DCD configuration
x_o	7 μm	7 μm
y_o	7 μm	7 μm
θ_o	0.05 mrad	0.1 mrad
Φ_o	0.1 mrad	0.05 mrad
δ_o	0.008%	0.016%

3.2   Parasitic aberrations

Parasitic aberrations are produced by the misalignment of the magnets. The misalignment contains magnet transverse translations, tilts around the x and y axis, rotation around the beam optical axis and percentage change in the excitation. In addition, mechanical imperfections during production also cause parasitic aberrations. To minimize the influence of the parasitic aberrations, the quadrupole triplet is fabricated into a monobloc triplet and treated as a whole in the misalignment simulation. Fig. 4 shows the geometrical aberrations applied to this monobloc quadrupole triplet. Table 3 shows the predictions of

the parasitic aberration coefficients for the IMP microbeams with the displacement on target less than 100 nm calculated by the TRANSPORT code. It appears that a minimum precision for the monobloc triplet of 0.25 μm in translations (U, V) or 0.0009 mrad in tilts (α, β) is required as well as a field tolerance of 10^{-4}.
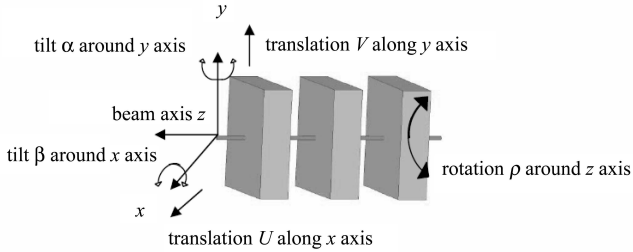

Fig. 4. Description of the misalignment parameters applied to the monobloc quadrupole triplet in the calculation of the parasitic aberration coefficients.

Table 3. Parasitic aberration coefficients of the monobloc triplet of the IMP microbeam system.

	coefficient	precision
D_x	15.19	-
D_y	-15.20	-
$\langle x\|U\rangle$	0.32 μm/μm	0.25 μm
$\langle y\|V\rangle$	0.32 μm/μm	0.25 μm
$\langle x\|\alpha\rangle$	62.50 μm/mrad	1.6 μrad
$\langle y\|\beta\rangle$	111.11 μm/mrad	0.9 μrad
$\langle x\|\Phi\rho\rangle$	0.45 μm/mrad^2	2.0 mrad
$\langle y\|\theta\rho\rangle$	0.40 μm/mrad^2	4.0 mrad
$\langle x\|\theta\varepsilon_1\rangle$	40.00 μm/mrad%	0.04%
$\langle x\|\theta\varepsilon_2\rangle$	-160.00 μm/mrad%	-0.01%
$\langle x\|\theta\varepsilon_3\rangle$	-28.57 μm/mrad%	-0.07%
$\langle y\|\Phi\varepsilon_1\rangle$	53.33 μm/mrad%	0.015%
$\langle y\|\Phi\varepsilon_2\rangle$	-32.00 μm/mrad%	-0.025%
$\langle y\|\Phi\varepsilon_3\rangle$	20.00 μm/mrad%	0.04%

4   Experiment platform

The IMP microbeam system is to serve both material experiments and biological experiments. There is an innovative design of the vertical vacuum chamber for material irradiation experiments. Some apparatus, such as the optical microscope, the ion detector and the moveable sample stage, are used to detect the single ion hit and online observation of the irradiation effects. Moving the sample stage in the vacuum chamber can facilitate the beam to pass through the vacuum window into the atmosphere instead of removing the vacuum chamber when doing the biological experiments. So a silicon nitride window is provided not only for the beam extraction but also for the beam detection. This silicon nitride vacuum window, covered with Au and CsI, also acts as the secondary electron detector together with a channeltron. When any particle passes through the vacuum window, the surface of the vacuum window produces the electron cloud so that the ion is detected and counted. The biology irradiation is composed of the fluorescent microscope, hypersensitivity CCD, the high precision moveable holder, the cell dish and so on.

5   Discussions

The TRANSPORT and MULE codes agree very well in the first order ion beam optics. For comparison, TRANSPORT from PSI[17] is also used to calculate all of the above results, and they are identical to the results by TRANSPORT from PBO-LAB when the precision of input is the same.

From Fig. 3, the final image can be further improved by reducing the object slit and divergence defining slit at the cost of fewer particles. The divergence defining slit defines the divergence angle and the momentum spread simultaneously. Though the chromatic aberrations have more influence than the spherical aberrations on the final beam spot size, there is no necessity to use sextupoles to correct the second order aberrations owing to the energy analyzer. The beam position is very sensitive to the stability of the two dipole magnets, which is very important to the IMP microbeam line. To minimize the displacement of the beam centroid, a tolerance of 10^{-5} is required for the power supply of the dipoles. Besides, the field tolerance of 10^{-3} for the quadrupole between the two dipole magnets is enough for this microbeam.

High energy is a particular advantage for the IMP microbeam system, but the damage of the slits or apertures associated with it is inevitable. So a coarse slit made up of tungsten carbide is preset before the object slit to protect it. The maximum current intensity for SFC is 10 μA, so the corresponding particles per second for this microbeam system are more than 1500. According to the simulations in this paper, a designed beam spot size of 1 μm in vacuum and 2 μm in atmosphere can be attained, and the particles per second can also be ensured to be more than 1000.

6   Outlooks

Presently, the φ80 quadrupole magnets, the dipole magnets, the corrector magnets and the scan-

ning system are all moved to the microbeam assembly line. One of the high gradient $\phi15$ quadrupoles has been accomplished, and the quadrupole triplet will be sent to Lanzhou by the end of this mouth. The vacuum system has completed its contracts and the corresponding tests. The power supply system is testing all its control boxes now. In addition, the instruments for the diagnosis and experiment are also arriving in Lanzhou gradually. The microbeam line will be installed in August.

Then some elementary measurements will be done on it to check the performance of the IMP microbeam system, such as scanning a copper micro-grid, writing a regular 10×10 point pattern onto a CR-39 track detector and so on. Further, some low-dose, sub-cellular target and "non-targeted" irradiations will be carried out to study the bystander effects,

genomic instability, the DNA damage and the cell-to-cell communications. In addition, some special new experiments have been designed for the IMP high energy heavy ion microbeam, for example, irradiating the plant cells and the specific semi-conductor device. It is believed that the IMP high energy heavy ion microbeam will open up a new fascinating research field.

References

1 Brown K A, Flliler R, LI Zheng et al. http://www.pubs.bnl.gov/documents/24105.pdf

2 Kobayashi Y, Funayama T, Wada S et al. Biol. Sci. Space, 2004, **18**(4): 235

3 Hirao T, Mori H, Laird J S et al. Nucl. Instrum. Methods B, 2003, **210**: 227

4 Oikawa M, Kamiya T, Fukuda M et al. Nucl. Instrum. Methods B, 2003, **210**: 54

5 Moretto Ph, Michelet C, Balana A et al. Nucl. Instrum. Methods B, 2001, **181**: 104

6 Ryan C G, Jamieson D N. Nucl. Instrum. Methods B, 1999, **158**: 97

7 SONG Ming-Tao, SHENG Li-Na, WANG Zhi-Guang et al. Chinese Physics C (HEP & NP), 2008, **32**(SuppI): 259

8 Ziegler J F. Nucl. Instrum. Methods B, 2004, **219**—**220**: 1027

9 Dolinskii A, Beller P, Beckert K et al. http://accelconf.web.cern.ch/Accelconf/e02/PAPERS/THPLE076.pdf

10 Gillespie G H, Hill B W, Martono H et al. Nucl. Instrum. Methods B, 2000, **161**—**163**: 1168

11 Agostinelli S, Allison J, Amako K et al. Nucl. Instrum. Methods A, 2003, **506**: 250

12 Mutsaers P H A. Nucl. Instrum. Methods B, 1996, **113**: 323

13 Jamieson D N. Nucl. Instrum. Methods B, 2001, **181**: 1

14 Greif K D, Brede H J, Frankenberg D et al. Nucl. Instrum. Methods B, 2004, **217**: 505

15 Grime G W, Watt F, Blower G D et al. Nucl. Instrum. Methods, 1982, **197**: 97

16 Jamieson D N, Rout B, Szymanski R et al. Nucl. Instrum. Methods B, 2002, **190**: 54

17 Rohrer U. ftp://ftp.psi.ch/psi/transport.beam/